Original papers
Nanostructured, nanoscale materials and nanodevices

УДК 537.533.2; 535.375.54 DOI: 10.17277/jamt.2024.01.pp.023-036

Structural and field emission characteristics of carbon-containing cathodes

© Evgeny P. Sheshin[a]✉, Nataliya D. Kundikova[bc], Viktor B. Kireev[a], Kirill N. Belov[c], Fung Dyk Many[a], Alexey S. Berdnikov[c], Danila N. Prosekov[c]

[a] *Moscow Institute of Physics and Technology (NRU), 9, Institutsky Lane, Dolgoprudny, 141701, Russian Federation;*
[b] *Institute of Electrophysics, Ural Branch of the Russian Academy of Sciences, 106, Amundsen St., Ekaterinburg, 620016, Russian Federation;*
[c] *South Ural State University (NRU), 76, Lenin Av., Chelyabinsk, 454080, Russian Federation*

✉ sheshin.ep@mipt.ru

Abstract: Field emission and structural characteristics of carbon nanotube fibers, polyacrylonitrile fibers, pyrolytic graphite and micrograined dense graphite were experimentally studied before and after their operation as a field emission cathode using registration of the current-voltage characteristics, optical microscopy, scanning electron microscopy and Raman spectroscopy in the spectral range from 1000 to 2000 cm^{-1}. The experiments showed large and small structural rearrangements of carbon-containing cathodes and their surfaces in the process of field emission. In addition to lines of the Raman spectra with frequency maxima in the known ranges: *G* (1581–1599 cm^{-1}), *D* (1363–1374 cm^{-1}) and *D′* (1619–1626 cm^{-1}), characteristic of carbon materials, a line was detected in the range 1450–1480 cm^{-1}, which is observed in the starting materials of pyrolytic graphite, carbon nanotube fibers and persists after operation, and also appears in a sample of micro-grained dense graphite after operation as a cathode. The relative integral intensity of line *D* in pyrolytic graphite, micrograined dense graphite, and carbon nanotube fibers undergoes the greatest change. In pyrolytic graphite and carbon nanotube fibers its increase is observed, and in micrograined dense graphite its decrease is observed after operation as a cathode. This made it possible to use the relative integral intensity of the *D*-line to quantify the change in the surface properties of carbon materials as a result of field emission when using these materials as cathodes, in particular to assess changes in crystallite sizes. Thus, the possibility of using Raman spectra to control the surface structure of carbon-containing materials has been demonstrated, which significantly facilitates the possibility of further analysis of the relationship between the surface structure and its emission characteristics. The prospects for improving the field emission characteristics of carbon-containing cathodes were discussed.

Keywords: field emission; field emission cathode; field emission current; volt-ampere characteristics; optical microscopy; raster (scanning) electron microscopy; Raman spectra; carbon-containing materials; nanostructured materials; surface structure.

For citation: Sheshin EP, Kundikova ND, Kireev VB, Belov KN, Many Fung Dyk, Berdnikov AS, Prosekov DN. Structural and field emission characteristics of carbon-containing cathodes. *Journal of Advanced Materials and Technologies*. 2024;9(1):023-036. DOI: 10.17277/jamt.2024.01.pp.023-036

Структурные и автоэмиссионные характеристики углеродсодержащих катодов

© Е. П. Шешин[a]✉, Н. Д. Кундикова[bc], В. Б. Киреев[a], К. Н. Белов[c], Фунг Дык Мань[a], А. С. Бердников[c], Д. Н. Просеков[c]

[a] *Московский физико-технический институт (НИУ), Институтский пер., 9, Долгопрудный, 141701, Российская Федерация;*
[b] *Институт электрофизики УрО РАН, ул. Амундсена, 106, Екатеринбург, 620016, Российская Федерация;*
[c] *Южно-Уральский государственный университет (НИУ), пр. Ленина, 76, Челябинск, 454080, Российская Федерация*

✉ sheshin.ep@mipt.ru

Аннотация: Проведено сопоставление автоэмиссионных и структурных характеристик поверхностей ряда углеродсодержащих, в том числе и наноструктурированных материалов, перспективных для использования при создании автокатодов со стабильными эмиссионными характеристиками. Исследовались волокна из углеродных

нанотрубок (УНТ-волокно), полиакрилонитрильные волокна, образцы пиролитического графита и мелкозернистого плотного графита (МПГ-6). Структура поверхности образцов исследовалась до и после их работы в качестве автокатода с использованием оптической микроскопии, растровой электронной микроскопии и спектроскопии комбинационного рассеяния. Эти результаты сопоставлялись с вольтамперными характеристиками соответствующих катодов. Оптическая и электронная микроскопия показали наличие крупномасштабных, а анализ спектров комбинационного рассеяния (СКР) – мелкомасштабных структурных перестроек катода и поверхности его материалов в процессе автоэмиссии. В спектральном диапазоне от 1000 до 2000 $см^{-1}$ в СКР кроме стандартно наблюдаемых характерных для углеродсодержащих материалов линий с максимумами частот в диапазонах 1363…1374 $см^{-1}$ (линия *D*), 1581…1599 $см^{-1}$ (линия *G*), 1619…1626 $см^{-1}$ (линия *D′*) обнаружена линия в интервале 1450…1480 $см^{-1}$ для пиролитического графита и УНТ-волокна – до и после эксплуатации, а для МПГ-6 – после эксплуатации этих материала в качестве автокатодов. Обсуждены изменения в СКР относительной интегральной интенсивности линии *D*, которая увеличивается для пиролитического графита и УНТ-волокна и уменьшается для МПГ-6 в процессе их эксплуатации в качестве автокатодов. Величина относительной интегральной интенсивности линии *D* использована для оценок размеров кристаллитов и их изменений в ходе автоэмиссии, что обосновывает возможность использования СКР для контроля структуры поверхности углеродсодержащих материалов и анализа связи структуры поверхности и ее эмиссионных характеристик. Обсуждены перспективы улучшения автоэмиссионных характеристик углеродсодержащих катодов.

Ключевые слова: автоэмиссия; автоэмиссионный катод; ток автоэмиссии; вольтамперная характеристика; оптическая микроскопия; растровая (сканирующая) электронная микроскопия; спектры комбинационного рассеяния; углеродсодержащие материалы; наноструктурированные материалы; структура поверхности.

Для цитирования: Sheshin EP, Kundikova ND, Kireev VB, Belov KN, Many Fung Dyk, Berdnikov AS, Prosekov DN. Structural and field emission characteristics of carbon-containing cathodes. *Journal of Advanced Materials and Technologies*. 2024;9(1):023-036. DOI: 10.17277/jamt.2024.01.pp.023-036

1. Introduction

The development and utilization of novel electrovacuum devices that leverage the field emission effect, encompassing diverse radiation sources like UV lasers [1], IR, visible, and UV cathodoluminescent lamps [2], as well as low-power X-ray tubes [3] for a range of applications, such as disinfection or the production of efficient X-ray radiation sources for various needs, appear to be highly pertinent. Indeed, the exploration of carbon-based (and nanostructured) materials for field emission cathodes is a promising area of research due to their unique electrophysical properties and potential applications in cathodoluminescent devices. In particular, the efficiency of the corresponding devices is greatly affected by the durability and stability of the emission characteristics of a number of carbon materials, which depend on the field emission modes that determine the structural changes of the emitting surface [4–6].

Since the type and parameters of nanostructures of the electron-emitting surface of carbon materials are crucial for their field emission characteristics, their evolution during field emission processes determines the dynamics of the field emission current change when a constant accelerating voltage is applied, and hence the stability of the operation of field emission devices based on carbon-containing materials. This makes it particularly relevant to study the surface changes of such materials during field emission and to identify the relationships between the surface structure and field emission characteristics of the corresponding carbon materials.

It is well known that along with various types of optical and electron microscopy, Raman spectroscopy can provide valuable information on the fine structure of carbon materials surfaces [7–22].

It should again be emphasised that the durability and stability parameters of field emission cathodes directly determine the competitiveness of new electrovacuum devices using the field emission effect, in particular, for radiation sources in various spectral ranges.

We have previously obtained expressions for the efficiency of the corresponding radiation sources of different types [2, 4, 5].

For example, for sources of visible, X-ray and UV radiation, the following ratio for the efficiency is valid:

$$Ef = \left(\frac{P}{S \times B} + \frac{P_{\text{el}}}{E \times D} \right) \equiv (A + B)^{-1}, \quad (1)$$

where *Ef* is the value of light radiation source efficiency equal to the ratio of useful effect (of light or energy flow) to total costs, including installation, operation and disposal costs; $A \equiv \frac{P}{S \times T}$; $B \equiv \frac{P_{\text{el}}}{E \times D}$; P is the sum of installation and disposal costs applied to one moment of time; S is the light flow in lumens (for

visible light sources) or energy in a given spectral range (for UV or X-ray sources); T is the continuous service life of the radiation source; P_{e1} is the cost per kWh of input energy in the absence of other operating costs; E is the light output (for visible light sources) or energy efficiency (for UV or X-ray sources); D is a discount factor reflecting the operating mode of the radiation source.

Estimates show that to ensure the competitiveness of general-purpose field emission light sources, a period of continuous stable operation of the radiation source – T must be ensured in the order of several tens of thousands of hours (preferably 50,000 hours and more).

This means that special attention should be paid to the issues of stable and long-term operation of field emission cathodes and identification of promising materials and modes of their operation. In particular, for carbon-containing materials of field emission cathodes, in the course of their operation during the emission of electrons, the structure of their surface and, together with it, the emission properties of the field emission cathode are changed and constantly renewed [2, 4–7].

This paper summarizes our results on the study of promising carbon-containing materials for field emission cathodes, including a comparative analysis of their field emission and structural characteristics, which can change during electron emission under different modes of field emission cathode operation.

The objective of the work was to compare the evolution of surface and field emission characteristics during the long-term process of electron field emission for different materials, namely to compare the experimentally obtained field emission characteristics of field emission cathodes and structural characteristics of the cathode and its surface using optical, scanning electron microscopy and Raman spectroscopy before and after long-term operation of the material as an field emission cathode. In addition to the new experimental results, we also used previously obtained results already published in [4–7].

2. Materials and Methods

2.1. Carbon materials for the field emission cathodes under study

In this work, as well as in [4–7], we used such nanomaterials as CNT filaments (carbon nanotube fibers) (FGBNU "TISNUM", Troitsk, Russia), with a diameter of about 30 μm, obtained by agglomeration of nanotubes; PAN-fibers (polyacrylonitrile fibers) ("Uglekhimvolokno", Mytishchi, Russia), which is a bundle of 200–300 polyacrylonitrile filaments each with a diameter of about 6 μm; and massive carbon materials (JSC NIIgraphite, Moscow, Russia): MPG-6 (high-strength fine-grained dense graphite) with a density of about 1.7 g·cm^{-3}, and pyrolytic graphite with a density of about 2.2 g·cm^{-3}.

2.2. Determining field emission characteristics of cathodes

The methods of preparation of cathodes from the investigated materials were described earlier [4–6]. The field emission characteristics were measured according to the two-electrode scheme in a vacuum chamber at a pressure of 10^{-6} Torr at a distance of 1 cm between the cathode from the investigated material and the anode, which is an electrode with a cathodoluminophore with a diameter (6.5 cm) significantly exceeding the dimensions of the emitting surface of the cathode (for different materials – cathodes with characteristic linear dimensions of the emitting surface from 1 to 6 mm).

When a positive voltage was applied to the anode, electrons were emitted from the cathode, and the current-voltage characteristics (CVC) and current-time dependencies were measured for different carbon-containing material cathodes.

2.3. Analysis of the structural characteristics of carbon-containing materials for field emission cathodes

The structural characteristics of the surface of carbon-containing field emission cathode materials and their evolution during electron emission were investigated using optical, scanning electron microscopy (SEM) and Raman spectroscopy.

Optical images of the surface of carbon-containing field emission cathode materials were recorded using an "Olympus" microscope, which allows obtaining digital images with magnification in the range up to 100× times. The magnifications of 5×; 10×; 20×; 50× and 100× times and the image sizes of the surface areas at the corresponding magnifications were used:

5× times – 2.8 × 2.2 mm;
10× times – 1.4 × 1.1 mm;
20× times – 700 × 550 μm;
50× times – 280 × 225 μm;
100× times – 140 × 112 μm.

Electron images of the microstructure of materials before and after their use as field emission cathodes were obtained at an accelerating voltage of 30 kV using a JEOL JSM 7001F scanning electron microscope in the same way as previously in [4–6].

The image field size of the scanning electron microscope using a focal length of 8 to 10 mm with sufficient image sharpness could vary in the range from 1 μm to several hundreds of μm.

This study continues the work presented in [7], using the same technique of obtaining and analysing Raman spectra using a ZNL Integra Spectra Raman spectrometer. Processing of the obtained Raman spectra was carried out using the software Fityk [8], which made it possible to extract individual lines of the spectrum assuming that the shape of each line is described by a Lorentz function, and to determine the maximum frequency, width and relative integrated intensity of each line of the spectrum in the frequency range 1000–2000 cm^{-1}. The characteristics of each line were determined at different background levels (at least three different levels), averaged with the estimation of maximum deviations from the mean values, which did not exceed 10 % for all experiments performed.

In this work, we have analysed in detail the spectral range of Raman spectra in the frequency range 1000–2000 cm^{-1}, which corresponds to the presence of the well-known *G*, *D* and *D′* lines [9, 10, 13–17] characteristic of carbon materials. It is also known that certain changes in the graphite structure of such materials are also reflected in the Raman spectra at frequencies around 2700 cm^{-1} [11]. However, no significant influence of auto-electron emission on the Raman spectra was found for the examined samples in this range and, therefore, it was decided to analyse in detail the line parameters in the Raman spectra in the frequency range 1000–2000 cm^{-1}, where we observed changes in the Raman spectrum as a result of using the examined samples as auto-electron emitters.

3. Results and Discussion

3.1. Structural and field emission characteristics of carbon-containing materials and cathodes made from them

3.1.1. Characteristics of fine-grained dense graphite MFG-6 and pyrolytic graphite

When recording the CVC of fine-grained dense graphite MPG-6 (curve *1* in Fig. 1) and pyrolytic graphite (curve *2* in Fig. 1), it was shown [6] that the threshold electric field strength of field emission for different samples of both types of materials is close in value in the range of 3600–3800 $V \cdot cm^{-1}$. At the same time, already at electric field strength of about 4500 $V \cdot cm^{-1}$ the value of field emission current density per unit of the emitting surface of the cathode for pyrolytic graphite exceeds several times the value of field emission current density for fine-grained dense graphite MFG-6. Examples of CVCs for samples of field emission cathodes made of fine-grained dense graphite MFG-6 and pyrolytic graphite with approximately the same areas of electron-emitting surfaces were published earlier in [6].

For microscopic inspection and registration of Raman spectra for each of the materials several observation points were selected. An example of the choice of points for recording the RMS for different samples of fine-grained dense graphite MFG-6 is presented in Fig. 1.

For microscopic inspection and recording of Raman spectra for each of the materials several observation points were selected. An example of the choice of points for recording the Raman spectra for different samples of fine-grained dense graphite MPG-6 is presented in Fig. 1.

It should be noted that for different registration points for both MPG-6 and pyrolytic graphite samples, although there are some differences in the images (optical and electronic photographs) of the surface, but no pronounced structural rearrangements before and after the emission processes can be detected, while for Raman spectra such differences are undoubtedly observed, which may indicate some heterogeneity of the surface of the initial materials, and possible heterogeneity of the structures of the surfaces of the materials after their work as field emission cathodes. This may be caused not only by the initial differences, but also by possible differences (inhomogeneities) formed in the course of structural changes of the material surface in the process of electron field emission (differences in the dynamics of structural changes for different parts of the surface).

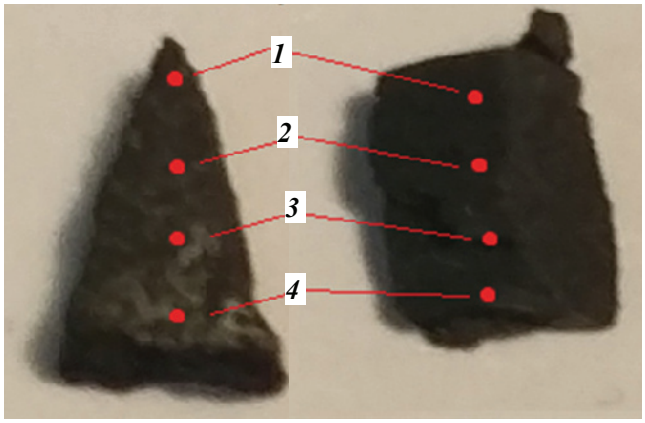

Fig. 1. Different samples of MPG-6:
on the left – sample used as an field emission cathode,
on the right – unused as an field emission cathode

Figures 2 and 3 show photographs, and Figs. 4, 5 show Raman spectra for different surface areas for fine-grained dense graphite MPG-6 (Figs. 2, 4) and pyrolytic graphite (Figs. 3, 5) before use as field emission cathodes and for samples of these materials already used as field emission cathodes.

Images of the surfaces of fine-grained dense graphite and pyrolytic graphite (Fig. 6) obtained by scanning electron microscopy also showed no significant differences for the different recording points both before and after the use of these materials as field emission cathodes. A typical view of the surfaces of these materials is presented in Fig. 6 (see also [4–6]).

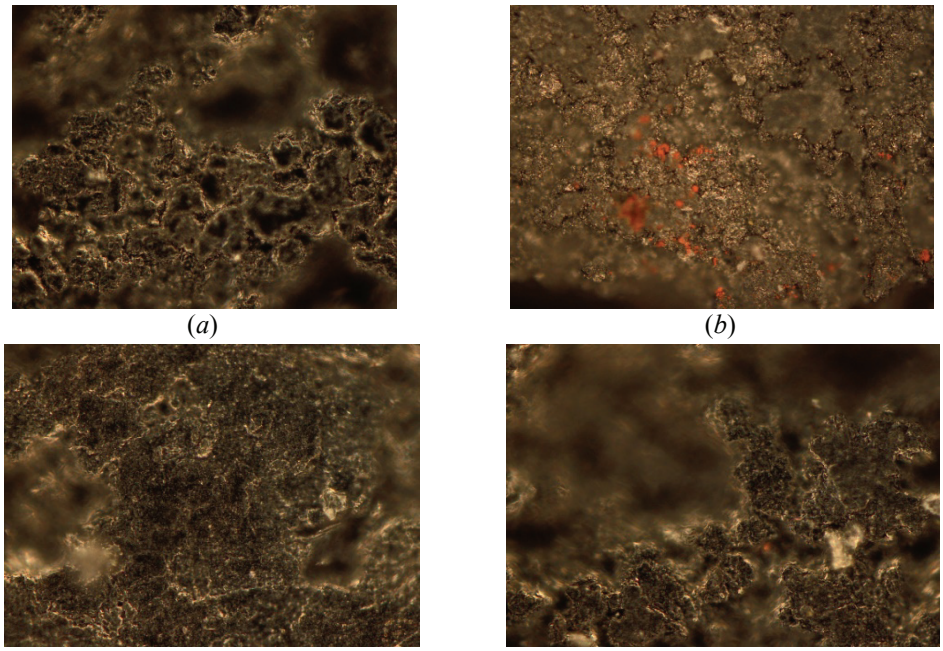

(*a*) (*b*) (*c*) (*d*)

Fig. 2. Surface views at 50× magnification of different sections of MPG-6 samples before use as an field emission cathode (*a*) and after use as an field emission cathode (*b*, *c*, *d*). Surface image size 280 × 225 μm

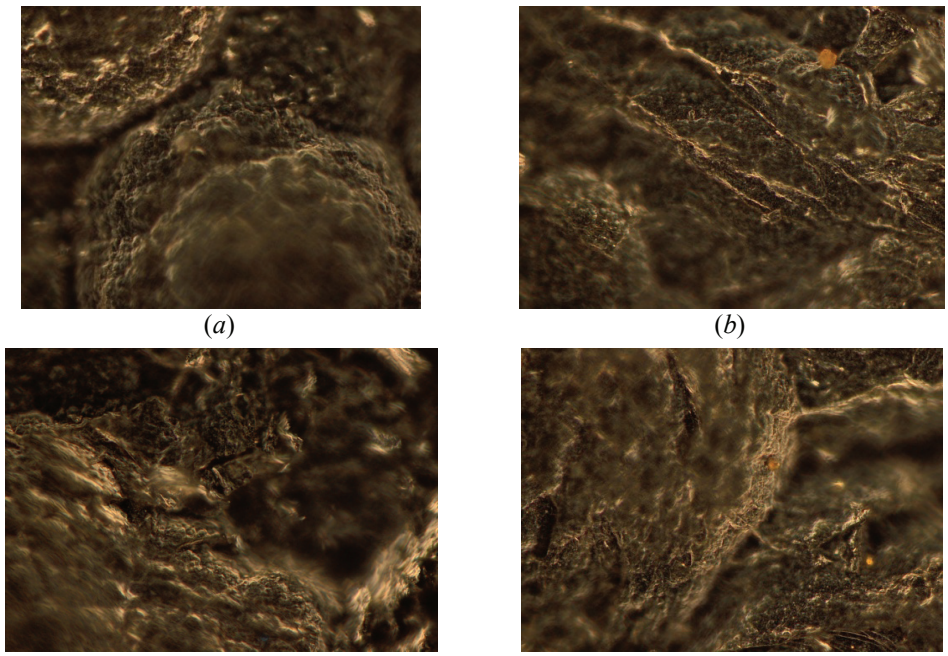

(*a*) (*b*) (*c*) (*d*)

Fig. 3. Surface view at 50× magnification of different sections of pyrolytic graphite samples before use as an field emission cathoede (*a*) and after use as an field emission cathode (*b*, *c*, *d*). Surface image size 280 × 225 μm

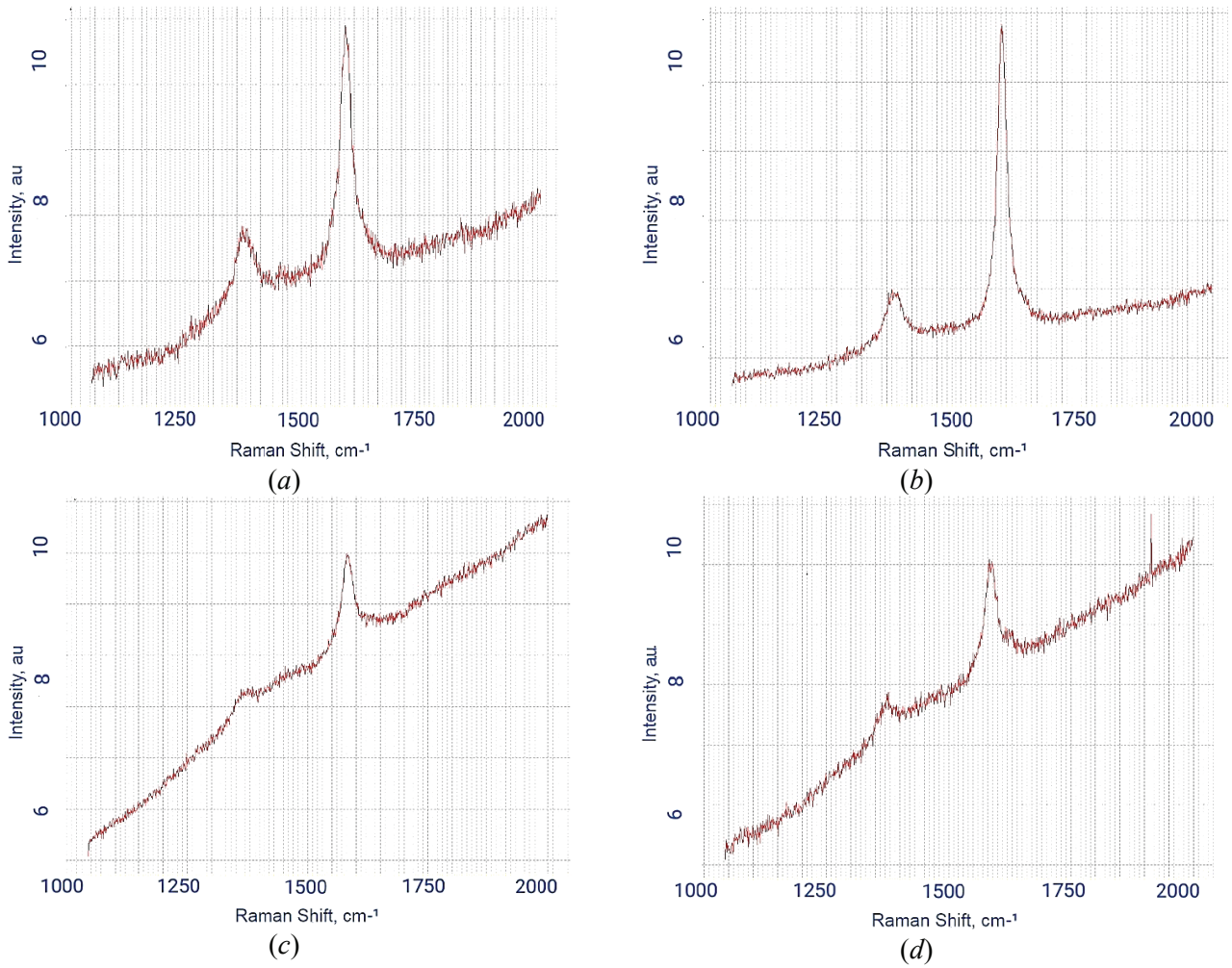

Fig. 4. Raman spectra of different sections of samples of fine-grained dense graphite MPG-6 before use as an field emission cathode (*a*, *b*) and after use as an field emission cathode (*c*, *d*) at points *1* (*a*, *c*) and 3 (*b*, *d*)

3.1.2. Characteristics of polyacrylonitrile fibers and carbon nanotube filaments

The structural and current-voltage characteristics of cathodes made of nanocarbon fibers and polyacrylonitrile fibers and the dynamics of emission current variation in time at different accelerating voltages in a two-electrode circuit were investigated. The data obtained earlier [4–6] and refined in this work show that the threshold electric field strength of field emission for samples from polyacrylonitrile fibers ranges from 1600 to 1850 V·cm^{-1}, and for carbon nanotube filaments from 500 to 600 V·cm^{-1}. At the same time, for carbon nanotube cathodes the CVC with increasing accelerating voltages, the emission current grows much faster than for polyacrylonitrile fibers. Moreover, for carbon nanotubes at a constant accelerating field strength of about 1300–1400 V·cm^{-1} the emission current increases compared to the initial value by 2–2.5 times within an hour and remains stable for several subsequent hours. In contrast, for cathodes made of polyacrylonitrile fibers at different accelerating voltages above the threshold values, a drop in the emission current over time is observed either immediately or after some increase (in the time interval of about an hour) and relative stabilisation within two to three subsequent hours. Photographs of the surfaces of the corresponding electrode materials obtained by optical microscopy and Raman spectra of such materials as carbon nanotubes and polyacrylonitrile fibers before and after their operation as field emission cathodes are presented, respectively, in Figs. 7, 8.

The analysis of optically and SEM-recorded images of carbon nanotube cathodes and polyacrylonitrile fibers cathodes obtained in [4–6] and in this work show that as a result of long-lasting electron field emission during prolonged operation of cathodes made of these materials there is a well-observed structural rearrangement of the cathode as a whole (Figs. 7, 8) and of individual fibers (Figs. 9, 10, combined from the data of our publications [4–6]).

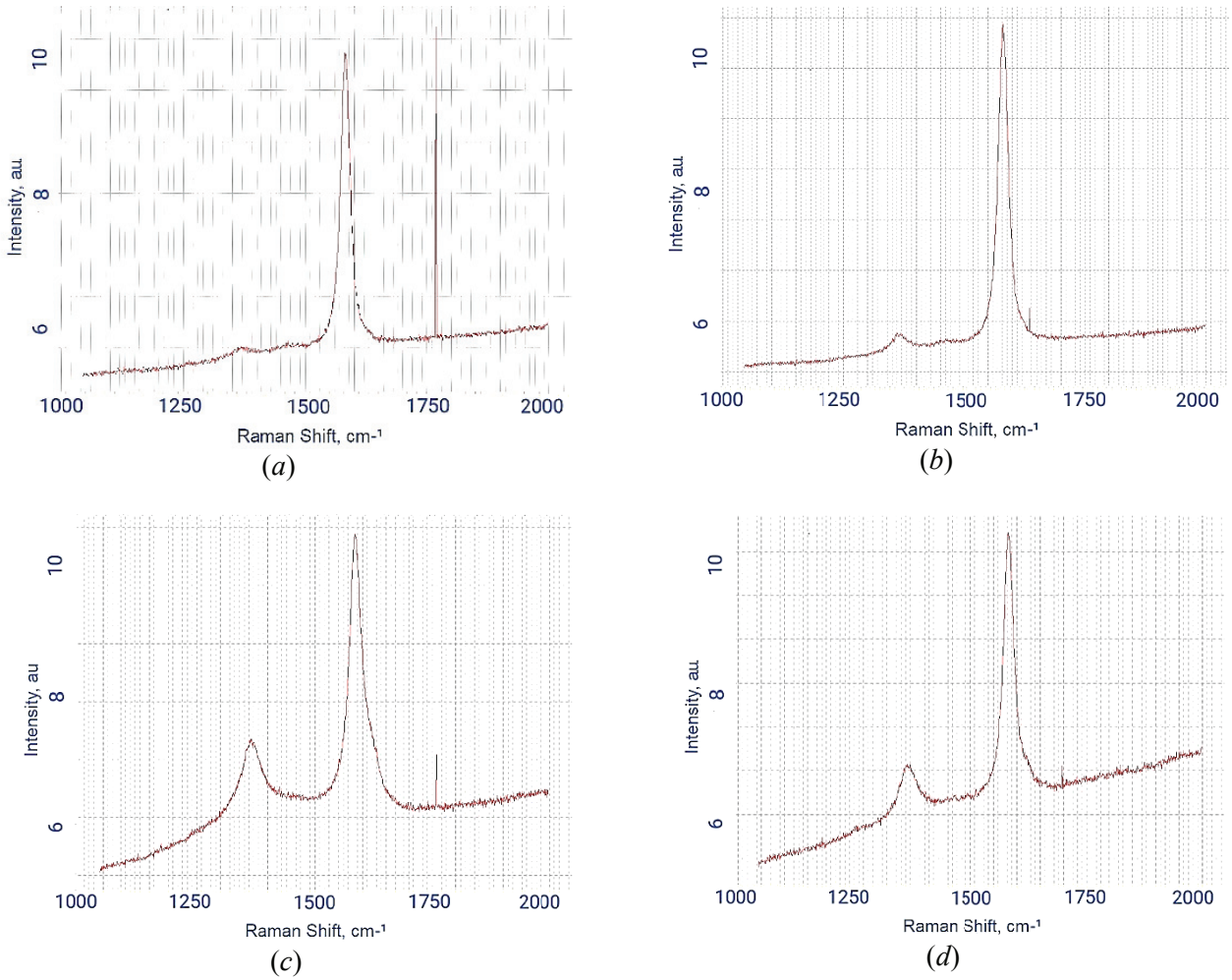

Fig. 5. Raman spectra of pyrolytic graphite samples before use as an field emission cathode (*a*, *b*) and after use as an field emission cathode (*c*, *d*) at points *1* (*a*, *c*) and *3* (*b*, *d*)

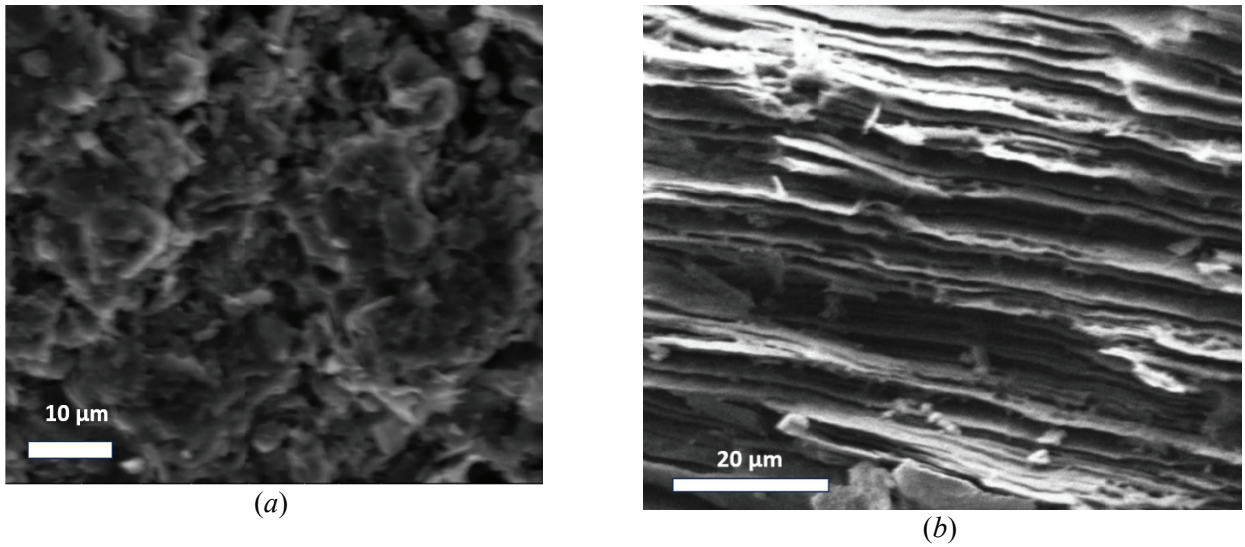

Fig. 6. Photos of cathode surfaces from arrays of fine-grained dense graphite MPG-6 (*a*) and pyrolytic graphite (*b*) obtained by SEM

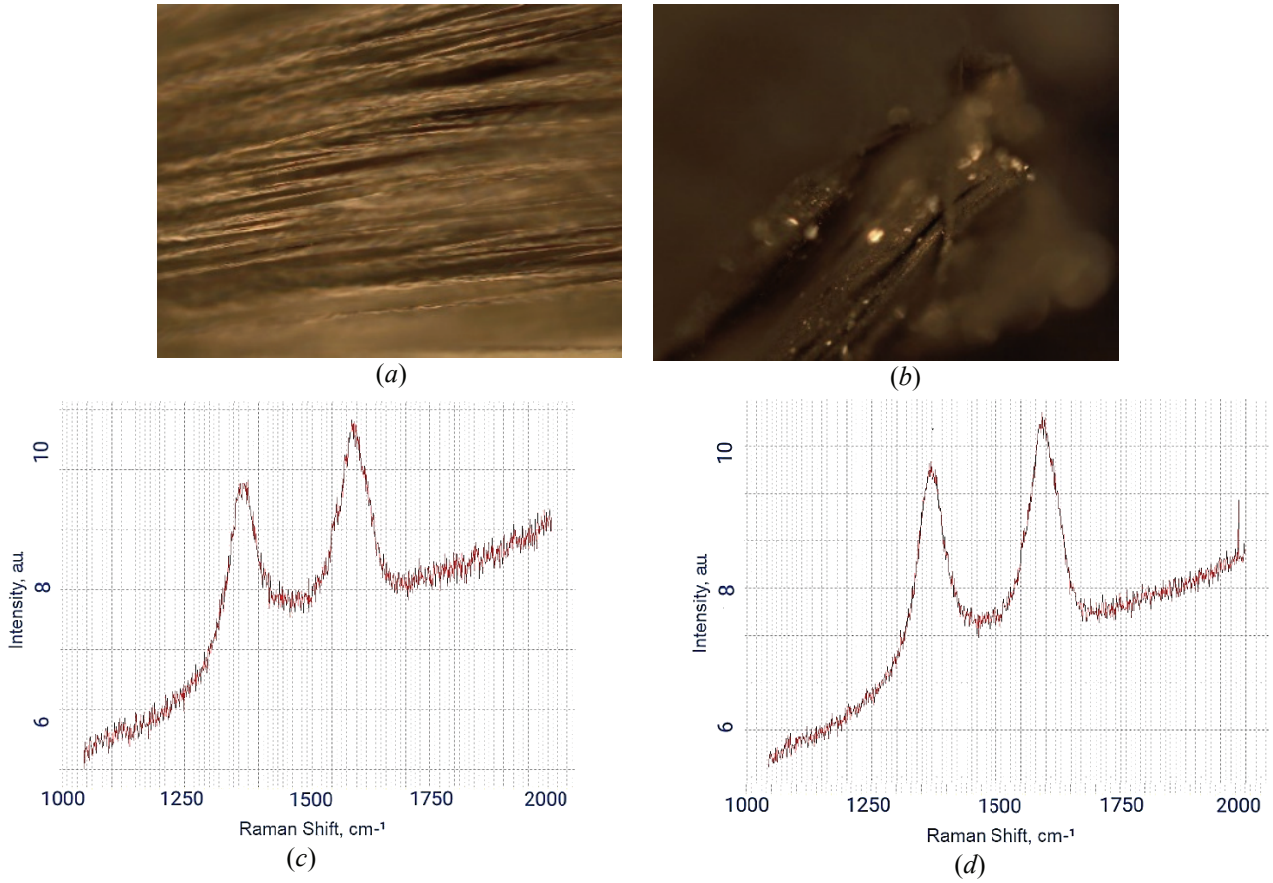

Fig. 7. Optical microscopy (*a* and *b*) (20× magnification) of a polyacrylonitrile fibers cathode and Raman spectra (*c* and *d*) of this fibers before (*a* and *c*) and after (*b* and *d*) its use as an field emission cathode material (The size of the surface section is 700 × 550 μm)

The images obtained by optical microscopy and SEM show that as a result of field emission processes polyacrylonitrile fibers melt, because during prolonged operation of these fibers as field emission cathodes at sufficiently high accelerating voltages they are heated above the melting point, which leads to their structural degradation and deterioration of their field emission properties. These conclusions are fully consistent with the above-described changes of the field emission current in time for field emission cathodes made of this material.

On the contrary, for the cathode based on carbon nanotube filaments, emission properties improve with time. This correlates well with the disordered structure of the field emission cathode and the destruction of carbon nanotubes during long-term field emission of electrons from this material, since a large number of new effective emission centers are apparently formed during disordered structure of the field emission cathode and destruction of carbon nanotubes. The change in the structure and the cathode itself and the structural rearrangement of the individual carbon nanotube are very well observed in the images of Figures 8 and 10, obtained by optical and scanning electron microscopy.

3.2. Discussion of the results obtained

The efficiency of using field emission cathodes in various electronic devices, and hence the relationship between field emission characteristics, operating modes and stability of field emission cathodes, especially those made of nanostructured carbon-containing materials, have been discussed in numerous publications, including [2–6, 23–30].

A comparison of the field emission characteristics of carbon-containing materials, in particular those studied in this work, demonstrates a certain inconsistency. On the one hand, cathodes made from arrays of carbon-containing materials such as fine-grained dense graphite MPG-6 and pyrolytic graphite have a threshold for the occurrence of emission current (the minimum electric field strength that ensures the occurrence of field emission current) significantly higher than that for cathodes made from nanostructured fibers, such like polyacrylonitrile fibers (about a three-fold difference) and especially for carbon nanotube filaments (about a six-fold difference).

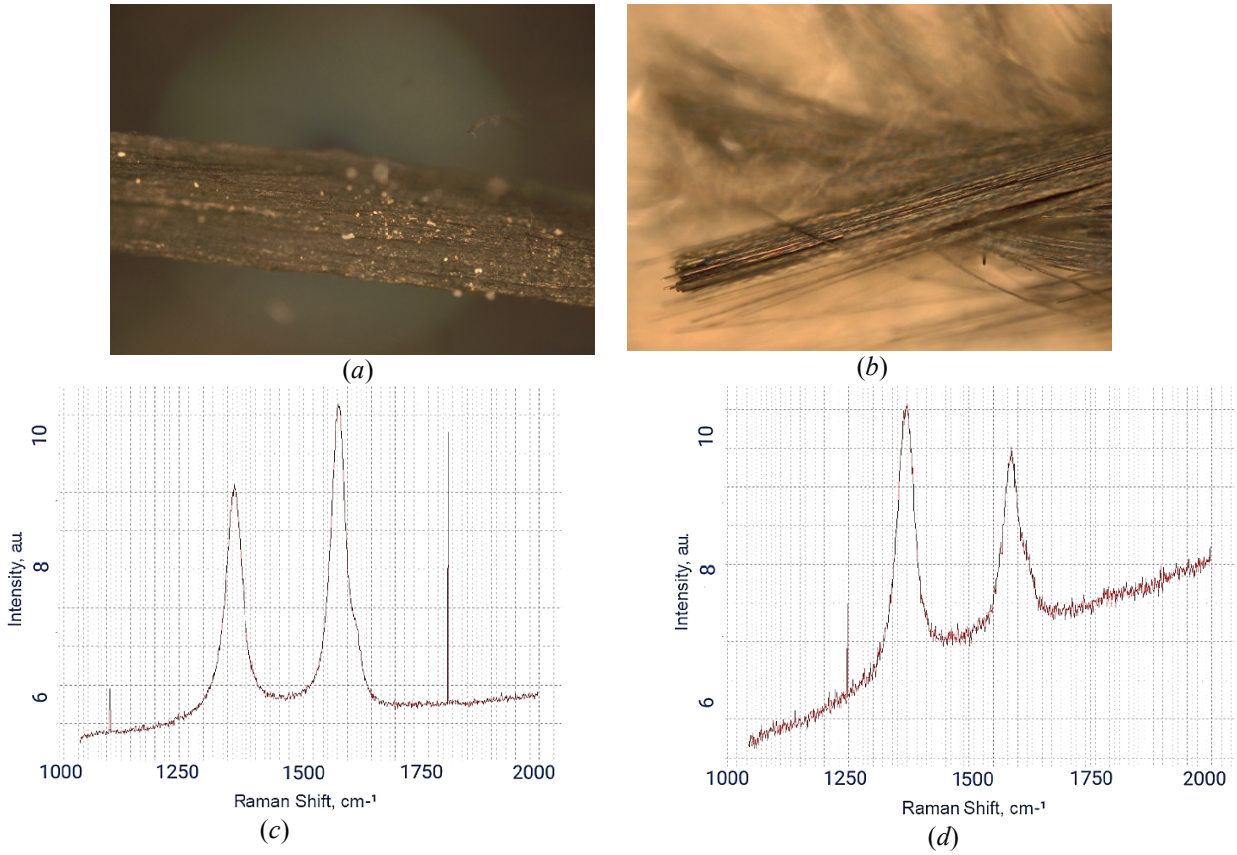

Fig. 8. Optical microscopy (*a* and *b*) (10× magnification) of carbon nanotube cathode and Raman spectra (*c* and *d*) for carbon nanotubes (CNT filaments) before (*a* and *c*), after (*b* and *d*) their use as an field emission cathode material (The size of the surface section is 1.4 × 1.1 mm)

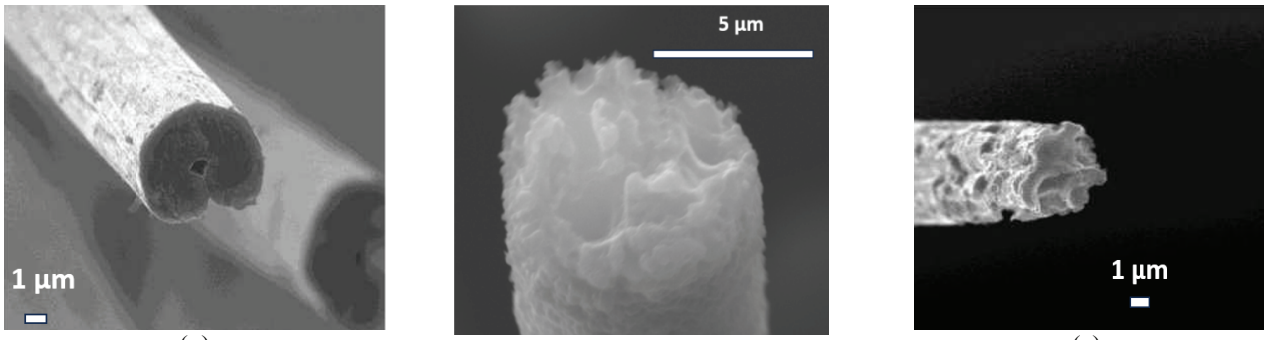

Fig. 9. SEM images of polyacrylonitrile fibers before (*a*) and after (*b*, *c* – at different emission process duration) the operation of fibers as part of the field emission cathode

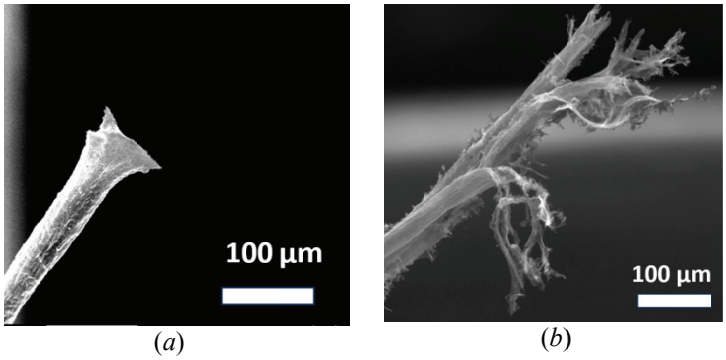

Fig. 10. SEM images of individual carbon nanotubes before (*a*) and after (*b*) the operation of these nanotubes as part of the field emission cathode

Table 1. Raman spectra data for samples of carbon-containing field emission cathode materials in the range 1000–2000 cm^{-1}

Peak, cm^{-1}	Pyrographite		PAN-fibers		MPG-6		CNT-fibers	
	before work	after work	before work	after work	before work	after work	before work	after work
D	1364.9	1366.8	1370.1	1373.2	1366.1	1366.8	1363.6	1367.6
X	1458.1	1458.5	NA	NA	NA	1454.8	1476.2	1462.5
G	1581.7	1584.7	1592.6	1599.0	1583.0	1583.5	1582.1	1586.4
D′	нет	1624.4	нет	нет	1616.9	1625.3	1619.8	1621.1

On the other hand, the field emission characteristics of massive cathodes made of carbon-containing materials are much more stable in a wide range of accelerating field strengths, although the field emission current for carbon nanotube filaments can be increased by an order of magnitude in a much narrower range of accelerating electric field strengths than even for the best of field emission cathode massive materials – pyrolytic graphite.

It should also be noted that although higher field emission current densities can be achieved for field emission cathodes made of nanostructured fibers, it is clear that at such current densities, macroscopic disturbances in the structure of both the nanofiber cathode itself and individual fibers occur.

For polyacrylonitrile fibers, this is melting and degradation of their field emission properties. For individual carbon nanotubes, these are numerous breaks, which, within the interval of several hours of operation of the field emission cathode, not only do not deteriorate its initial field emission properties, but can even improve them. This, however, does not guarantee the stability of the field emission cathode for tens of thousands of hours required for the effective operation of many field emission devices [2, 3].

When analyzing the Raman spectra, which records summary is presented in Table 1, the main Raman scattering lines in the range 1000–2000 cm^{-1} were considered. The maximum frequencies of the lines detected in the Raman spectra were obtained, as in our work [7], by averaging over all recording points of samples of the corresponding materials that were not used in the operation of field cathodes (in the table, the columns “before use”), and those used as field cathodes (in the table there are columns “after use”). In this work, with an increase in the number of samples and recording points in the studied samples in comparison with work [7], the characteristic values of the previously obtained frequencies of the maxima of the corresponding spectral lines were confirmed with an accuracy of 0.5 cm^{-1}, which corresponds to the instrumental accuracy of the Raman spectrometer “Integra Spectrum” with a diffraction grating of 1800 lines·mm^{-1}.

According to the results presented in Table 1, along with the well-known *G*, *D*, and *D′* lines [9, 10] characteristic of carbon materials, the following has been observed:

– *G* line with a maximum in the range 1581–1599 cm^{-1}, due to vibrations of carbon atoms in strongly bonded hexagonal planes;

– *D* line with a maximum in the range 1363–1374 cm^{-1}, caused by violations of translational symmetry in the studied materials;

– *D′* line with a maximum in the range 1619–1626 cm^{-1}, caused by disorder effects between carbon layers;

in the Raman spectra of samples of such materials as pyrographite, carbon nanotubes, and fine-grained dense graphite MPG-6, after use in an field emission cathode, a characteristic spectral line in the frequency range of 1450–1480 cm^{-1} was observed, labelled by us in the table, as well as in [7], the X-line. In [12], a similar line was observed in Raman spectra for samples of polyacrylonitrile fibers (unlike our data) and was associated with vibrations of the methylene group.

The frequencies of the maxima of the corresponding spectral lines and their insignificant shifts as a result of using the materials as field emission cathodes were briefly discussed earlier [7].

The most interesting observed effect from Raman spectroscopy data for the studied materials is the change in the relative integrated intensity of the *D* line with respect to the *G* line. In [9], the relative integrated intensity of the *D* line for fine-grained graphite is related to the size of its crystallites. The results of measuring the relative integral intensity of the *D* line before and after prolonged electron emission for all investigated samples of carbon-containing materials tested as materials for field emission cathodes are presented in Fig. 11.

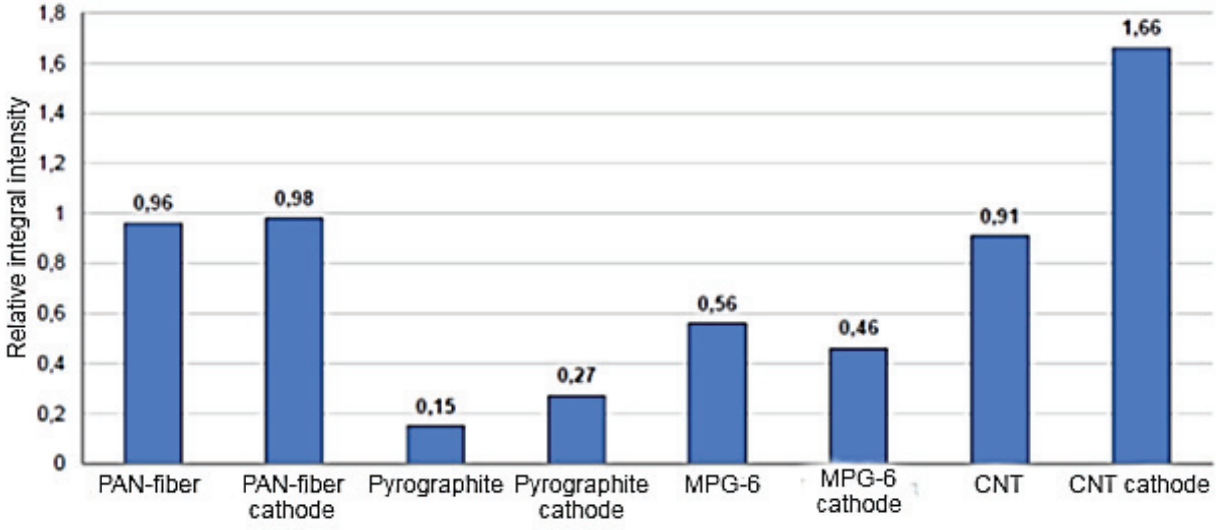

Fig. 11. Relative integral intensity of the *D* line before and after (cathode) long-term electron emission for all investigated samples of carbon-containing materials tested as materials for field emission cathodes

Voltampere characteristics and studies of current evolution over time show that a rather high current stability is observed in the range of voltages used for pyrolytic graphite and MPG-6, which is confirmed by relative macroscopic structural stability according to optical and scanning electron microscopy data. Nevertheless, the RSM data show that some small scale structural rearrangement occurs during operation of these materials, which is most likely related to the change in crystallite sizes.

The sizes of the average crystallites in this material before its operation as an field emission cathodes – 7.9 nm, and after – 9.6 nm – were estimated by the method proposed in [9] for fine-grained dense graphite using the data in Fig. 11.

Thus, the analysis of the relative integral intensity of the *D* line of Raman spectra of carbon materials allowed us to quantitatively estimate not only the average sizes of carbon crystallites in massive samples of MPG-6, but also the evolution of these sizes in the process of field emission.

Although the intensity of the *D* line in pyrographite is much lower than in fine-grained dense graphite MPG-6, it can be assumed that for this material the crystallite sizes are significantly smaller. This correlates with higher values of the field emission current under similar conditions and with the fact that pyrographite consists of layers of carbon crystallites, that pyrographite consists of layers with a thickness of about 1 μm, and the characteristic size of particles from which fine-grained dense graphite MPG-6 is compressed is about 50 μm, although, as our estimates show, the characteristic sizes of crystallites for these materials are much smaller. Moreover, the increase in the relative integral intensity of the D line as a result of prolonged electron emission may indicate for pyrographite a decrease in the size of emission centres during the operation of this material as an field emission cathode, although this question requires more detailed elaboration and additional studies.

The question of interpreting the significant increase in the relative integral intensity of the D line as a result of long-term electron emission for carbon nanotubes also remains open, since the legitimacy of applying the concept of crystallites to nanotubes raises some doubts. However, for fibers, structural analysis shows significant both large-scale and small-scale restructuring of the cathode and its surface. Moreover, PAN fiber sintering is observed in a number of modes, but for CNT fiber a strong macroscopic fiber disorder accompanied by the rupture of nanotubes and an improvement in field emission characteristics is characteristic, at least in a time interval of several hours.

Moreover, for each of the materials studied, it is possible to select operating modes and design solutions (for example, providing effective heat removal for field emission cathodes made of polyacrylonitrile fibers, preventing overheating and melting of this material) allowing the use of these materials to create effective field emission devices.

Of particular importance in this case is the study of their field emission characteristics, the dynamics of their changes and the associated structural rearrangements of their surface under various operating conditions of these materials as field cathode materials. Without knowledge of these characteristics, it is impossible to select appropriate operating modes that ensure the efficient use of these

materials in the creation of new field emission devices and devices.

Obtaining data on the field emission and structural characteristics of the surface of carbon-containing materials for field emission cathodes creates good prerequisites for optimizing the operation of field emission cathodes created on the basis of various carbon-containing materials, in particular, the use of a three-electrode circuit allows for various materials to provide the necessary field emission current by appropriately changing the voltage and distance between the cathode and mesh. By changing the shape, size of the cathode area, and the mode of excitation of the emission current, it is possible to provide the necessary density of this current, which allows avoiding excessive overheating and the occurrence of unacceptable mechanical stresses leading to destruction of the structures of the cathode materials.

4. Conclusion

The results obtained indicate that for carbon-containing materials, when used as field emission cathodes, both macroscopic and microscopic structural changes of the cathodes themselves and their surfaces occur, depending on the type of material and the mode of its operation. It is shown that measuring the relative integral intensity of the D line in Raman spectra makes it possible to evaluate the nature of the evolution of emission electron centers, and in some cases to estimate not only the sizes of carbon crystallites, but also the change in these sizes during the field emission process. It was found that for MPG-6 samples before and after using this material as the cathode of a field emission light source, the average crystallite size is different, and according to estimates, it is approximately 8 nm and 10 nm, respectively. The results obtained justify the possibility of using optical and scanning electron microscopy methods and methods of analyzing Raman spectra for a detailed study of the structure of field emission cathodes made of carbon materials and their surfaces, including the possibility of studying changes in their structure under different modes of their operation as cathodes of field emission radiation sources.

5. Funding

This study received no external funding.

6. Conflict of interests

The authors declare no conflict of interest.

References

1. Jmerik V, Kozlovsky V, Wang X. Electron-beam-pumped UVC emitters based on an (Al,Ga)N material system. *Nanomaterials*. 2023;13:1-42. DOI:10.3390/nano13142080

2. Bugaev AS, Kireev VB, Sheshin EP, Kolodyazhnyj AJ. Cathodoluminescent light sources: status and prospects. *Physics-Uspekhi*. 2015;58(8):792-818. DOI:10.3367/UFNe.0185.201508e.0853

3. Bugaev AS, Eroshkin PA, Romanko VA, Sheshin EP. Low-power X-ray tubes (the current state). *Physics-Uspekhi*. 2013;56(7):691-703. DOI:10.3367/UFNe.0183.201307c.0727

4. Kireev VB, Sheshin EP. Nanomaterials for effective auto-emission cathodoluminescent disinfecting light sources. *Scienceosphere*. 2022;4(1):1-12. DOI:10.5281/zenodo.6390489 (In Russ.)

5. Taikin AYu, Savichev IA, Popov MA, Anokhin EM, et al. Comparison and analysis of field emission characteristics of carbon cathodes based on PAN fiber and CNT filaments. *Journal of Advanced Materials and Technologies*. 2022;7(1):46-57. DOI:10.17277/jamt.2022.01.pp.046-057

6. Kireev VB, Sheshin EP. Field emission cathodoluminescent lamps: II. Nanostructured materials for field emission cathodes. *In Malkova MYu. (ed.) Engineering systems-2022: Proceedings of the International Conference. Engineering Systems-2022, 6-8 April 2022, Moscow,Russia*. Peoples' Friendship University of Russia; 2022. p.56-66. (In Russ.)

7. Belov KN, Berdnikov AS, Kireev VB, Kundikova ND, et al. Raman spectra of carbon materials used as cathodes of field emission radiation sources. *Bulletin of SUSU. Series "Mathematics. Mechanics. Physics"*. 2023;15(2):230206(41-47) DOI:10.14529/mmph230206 (In Russ.)

8. Wojdyr M. Fityk: A general-purpose peak fitting program. *Journal of Applied Crystallography*. 2010;43:1126-1128. DOI: 10.1107/S0021889810030499

9. Jawhari T, Roid A, Casado J. Raman spectroscopic characterization of some commercially available carbon black materials. *Carbon*. 1995;33(11):1561-1565.

10. Bokobza L, Bruneel J-L, Couzi M. Raman spectroscopy as a tool for the analysis of carbon-based materials (highly oriented pyrolitic graphite, multilayer graphene and multiwall carbon nanotubes) and of some of their elastomeric composites. *Vibrational Spectroscopy*. 2014;74:57-63. DOI:10.1016/j.vibspec.2014.07.009

11. Komlenok M, Kurochitsky N, Pivovarov P, Rybin M, Obraztsova E. Field electron emission from crumpled CVD graphene patterns printed via laser-induced forward transfer. *Nanomaterials*. 2022;12(11):1-8. DOI:10.3390/nano12111934

12. Panapoy M, Dankeaw A, Ksapabutr B. Electrical conductivity of PAN-based carbon nanofibers prepared by electrospinning method. *Thammasat International Journal of Science and Technology*. 2008;13:11-17.

13. Dyachkova TP, Khan YA, Burakova EA, Galunin EV, et al. Characteristics of epoxy composites containing carbon nanotubes/graphene mixtures. *Polymers (Basel)*. 2023;15(6):1-20. DOI:10.3390/polym15061476

14. Pimenta MA, Dresselhaus G, Dresselhaus MS, Cançado LG, et al. Studying disorder in graphite-based systems by Raman spectroscopy. *Physical Chemistry Chemical Physics*. 2007;9:1276-1290. DOI:10.1039/B613962K

15. Keszler AM, Nemes L, Ahmad SR, Fang X. Characterisation of carbon nanotube materials by Raman spectroscopy and microscopy – A case study of multiwalled and singlewalled samples. *Journal of Optoelectronics and Advanced Materials*. 2004;6:269-1274.

16. Hayashida K, Nagaoka S, Ishitani H. Growth and oxidation of graphitic crystallites in soot particles within a laminar diffusion flame. *Fuel*. 2014;128:148-154. DOI:10.1016/j.fuel.2014.03.008

17. Malard M, Pimenta MA, Dresselhaus G, Dresselhaus MS. Raman spectroscopy in graphene. *Physics Reports*. 2009;473:51-87. DOI:10.1016/j.physrep.2009.02.003

18. Gorelik VS, Sushchinskiĭ MM. Raman scattering of light in crystals. *Soviet Physics Uspekhi.* 1969;12:399-429. DOI:10.1070/PU1969v012n03ABEH003897

19. Kudelski A. Analytical applications of Raman spectroscopy. *Talanta*. 2008;76(1):1-8. DOI:10.1016/j.talanta.2008.02.042

20. Gorelik VS, Skrabatun AV, Bi D. Raman scattering of light in diamond microcrystals. *Crystallography Reports*. 2019;64:428-432. DOI:10.1134/S106377451903009X

21. Moris-Muttoni B, Raimbourg H, Champallier R, Augier R, et al. The effect of strain on the crystallinity of carbonaceous matter: Application of Raman spectroscopy to deformation experiments. *Tectonophysics*. 2023;869(230126):1-24. DOI:10.1016/j.tecto.2023.230126

22. Gibson RF, Ayorinde EO, Wen Y.-F. Vibrations of carbon nanotubes and their composites: A review. *Composites Science and Technology*. 2007;67(1):1-28. DOI:10.1016/j.compscitech.2006.03.031

23. Saito Y, Uemura S. Field emission from carbon nanotubes and its application to electron sources. *Carbon*. 2000;38(2):169-182. DOI: 10.1016/S0008-6223(99)00139-6

24. Wang ZL, Gao RP, De Heer WA, Poncharal P. In situ imaging of field emission from individual carbon nanotubes and their structural damage. *Applied Physics Letters*. 2002;80(5):856-858. DOI:10.1063/1.1446994

25. Silva SRP, Carey JD, Guo X, Tsang WM, Poa CHP. Electron field emission from carbon-based materials. *Thin Solid Films*. 2005;482(1–2):79-85. DOI:10.1016/j.tsf.2004.11.122

26. Le Normand F, Cojocaru CS, Fleaca C, Li JQ, et al. A comparative study of the field emission properties of aligned carbon nanostructures films, from carbon nanotubes to diamond. *The European Physical Journal Applied Physics*. 2007;38(2):15-27. DOI:10.1051/epjap:2007052

27. Kaur G, Pulagara NV, Kumar R, Lahiri I. Metal foam-carbon nanotube-reduced graphene oxide hierarchical structures for efficient field emission. *Diamond and Related Materials*. 2020;106:1-10. DOI:10.1016/j.diamond.2020.107847

28. Dwivedi N, Dhand C, Carey JD, Anderson EC, et al. The rise of carbon materials for field emission. *Journal of Materials Chemistry C*. 2021;9(8):620-659. DOI:10.1039/d0tc05873d

29. Ma Z, Li D, Zhang H, Wurz P, et al. Study of a low-energy collimated beam electron source and its application in a stable ionisation gauge. *Vacuum*. 2023;215:1-7. DOI:10.1016/j.vacuum.2023.112302

30. Xiao D, Du H, Sun L, Suo X, et al. Boosting the electron beam transmittance of field emission cathode using a self-charging gate. *Nature Communications*. 2024;15(764):1-10. DOI:10.1038/s41467-024-45142-0

Information about the authors / Информация об авторах

Evgeny P. Sheshin, D. Sc. (Phys. and Math.), Professor, Deputy Head Department of Vacuum Electronics, Head Laboratory of Vacuum and Microwave Electronics, Moscow Institute of Physics and Technology (National Research University) (MIPT), Moscow, Russian Federation; ORCID 0000-0003-2750-4797; e-mail: sheshin.ep@mipt.ru

Шешин Евгений Павлович, доктор физико-математических наук, профессор, заместитель заведующего кафедрой вакуумной электроники, заведующий лабораторией вакуумной и СВЧ-электроники, Московский физико-технический институт (Национальный исследовательский университет) (МФТИ), Москва, Российская Федерация; ORCID:0000-0003-2750-4797; e-mail: sheshin.ep@mipt.ru

Nataliya D. Kundikova, D. Sc. (Phys. and Math.), Professor, Head Department of Optoinformation, South Ural State University (National Research University) (SUSU), Chelyabinsk, Chief Researcher, Head Laboratory of Nonlinear Optics, Institute of Electrophysics, Ural Branch of the Russian Academy of Sciences, Ekaterinburg, Russian Federation; ORCID 0000-0002-5880-9393;e-mail: kundikovand@susu.ru

Viktor B. Kireev, Cand. Sc. (Phys. and Math.), Associate Professor, MIPT, Moscow, Russian Federation; ORCID 0000-0002-0699-2819; e-mail: kireev.vb@mipt.ru

Kirill N. Belov, Postgraduate, SUSU, Chelyabinsk, Russian Federation; ORCID 0009-0003-1915-5061; e-mail: belovkn@susu.ru

Fung Duc Man, Postgraduate, MIPT, Moscow, Russian Federation; e-mail: phungducmanh@phystech.edu

Alexey S. Berdnikov, Student, SUSU, Chelyabinsk, Russian Federation; e-mail: berdnikovas@susu.ru

Danila N. Prosekov, Student, SUSU, Chelyabinsk, Russian Federation; e-mail: prosekov97@mail.ru

Кундикова Наталия Дмитриевна, доктор физико-математических наук, профессор, заведующий кафедрой оптоинформатики Южно-Уральского государственного университета (Национальный исследовательский университет) (ЮУрГУ), Челябинск, главный научный сотрудник, заведующий лабораторией нелинейной оптики, Институт электрофизики УрО РАН, Екатеринбург, Российская Федерация; ORCID 0000-0002-5880-9393; e-mail: kundikovand@susu.ru

Киреев Виктор Борисович, кандидат физико-математических наук, доцент, МФТИ, Москва, Российская Федерация; ORCID 0000-0002-0699-2819; e-mail: kireev.vb@mipt.ru

Белов Кирилл Николаевич, аспирант, ЮУрГУ, Челябинск, Российская Федерация; ORCID 0009-0003-1915-5061; e-mail: belovkn@susu.ru

Фунг Дык Мань, аспирант, МФТИ, Москва, Российская Федерация; e-mail: phungducmanh@phystech.edu

Бердников Алексей Сергеевич, студент, ЮУрГУ, Челябинск, Российская Федерация; e-mail: berdnikovas@susu.ru

Просеков Данила Николаевич, студент, ЮУрГУ, Челябинск, Российская Федерация; e-mail: prosekov97@mail.ru

Received 13 December 2023; Accepted 16 February 2024; Published 26 April 2024